Available online at www.sciencedirect.com
ScienceDirect
International Journal of Thermal Sciences 46 (2007) 1033–1045
International Journal of Thermal Sciences
www.elsevier.com/locate/ijts

Effects of thin fin on natural convection in porous triangular enclosures

Yasin Varol [a], Hakan F. Oztop [b,*], Asaf Varol [c]

[a] *Department of Mechanical Engineering, Vanderbilt University, Nashville, TN 37235, USA*
[b] *Department of Mechanical Engineering, Firat University, TR-23119, Elazig, Turkey*
[c] *Department of Mechanical and Aerospace Engineering, West Virginia University, Morgantown, WV 26505, USA*

Received 18 August 2006; received in revised form 2 November 2006; accepted 3 November 2006

Available online 4 December 2006

Abstract

A two-dimensional solution of natural convection in solid adiabatic thin fin attached to porous right triangular enclosures has been analyzed numerically. The vertical wall of the enclosure is insulated while the bottom and the inclined walls are isothermal. The temperature of the bottom wall is higher than the temperature of the inclined wall. Governing equations, which are written using Darcy model, are solved via the finite difference technique. The Successive Under Relaxation (SUR) method was used to solve linear algebraic equations. Dimensionless location of the thin fin from 0.2 to 0.6, the aspect ratio of triangular enclosure from 0.25 to 1, Rayleigh number from 100 to 1000 and the dimensionless height of the fin from 0.1 to 0.4 are used as governing parameters that are effective on heat transfer and fluid flow. Results for the mean Nusselt number, velocity profiles, the contour maps of the streamlines and isotherms are presented. It is observed that the thin fin can use as a passive control element for flow field, temperature distribution and heat transfer.

Keywords: Porous medium; Triangular enclosure; Thin fin; Natural convection

1. Introduction

Natural convection heat transfer occurs in enclosures filled with porous medium as a result of temperature differences and buoyancy as observed in building insulation materials, cooling of electronical equipments, solar collectors, geothermal applications, oil destruction etc. These applications are reviewed in the literature by Nield and Bejan [1], Ingham and Pop [2].

Up to this date, natural convection was analyzed for different shaped enclosures. Geometrical shapes of enclosures can be classified in two categories as rectangular and non-rectangular shaped enclosures. Most of the researchers studied the rectangular or square shaped enclosures for air-filled [3–5] or porous medium filled [6–11] because of the simplicity of solutions for these geometrical shapes.

Some researchers investigated the effects of the geometric shapes on natural convection in enclosures such as triangle [12–18], parallelogram [19], trapezoidal [20–24], wavy [25,26] and so on. They showed that both flow and temperature fields are affected by the geometrical parameters.

A divider or partition can be used as a control parameter for heat transfer and fluid flow in enclosures. Many researchers studied the problem of divided rectangular or square non-porous enclosures with partition. The partition length, thickness and location centers are governing parameters for heat transfer as shown by Turkoglu and Yucel [27], Zimmerman and Acharya [28], Dagtekin and Oztop [29], Ben-Nakhi and Chamkha [30], Hasnaoui et al. [31], Yucel and Ozdem [32], Dagtekin et al. [33], Oosthuizen and Paul [34], Bilgen [35]. These studies are analyzed for rectangular or square shaped geometries and non-porous medium.

Tasnim and Collins [36] studied the natural convection in a square cavity with a thin baffle on the hot wall using finite-volume-method with collocated variable arrangement. They observed that the fin has a blocking effect on the fluid depending on the Rayleigh number, length of the baffle and its position, a number of recirculating regions can be formed above and under the baffle. Bilgen [37] solved the natural convection problem in cavities with a thin fin on a hot wall. He found that Nusselt

* Corresponding author. Tel.: +90 424 237 0000 ext. 5328; fax: +90 424 241 5526.
E-mail address: hfoztop1@yahoo.com (H.F. Oztop).

1290-0729/$ – see front matter
doi:10.1016/j.ijthermalsci.2006.11.001

Nomenclature

AR	aspect ratio, H/L	X, Y	non-dimensional coordinates
c	dimensionless fin position, c'/L	*Greek letters*	
g	gravitational acceleration ... $m\,s^{-2}$	υ	kinematic viscosity ... $m^2\,s^{-1}$
Gr	Grashof number	θ	non-dimensional temperature
h	dimensionless height of fin, h'/H	β	thermal expansion coefficient ... K^{-1}
H	height of triangle ... m	α	thermal diffusivity ... $m^2\,s^{-1}$
K	permeability ... m^2	Ψ	non-dimensional stream function
L	length of bottom wall of triangle ... m	*Subscript*	
Nu	Nusselt number	c	cold
Pr	Prandtl number	h	hot
Ra	Rayleigh number		
u, v	axial and radial velocities ... $m\,s^{-1}$		

number is an increasing function of Rayleigh number, and a decreasing function of fin length and relative conductivity ratio. Shi and Khodadadi [38] studied the almost perfectly conducting partition on the hot wall. Based on the obtained results, they proposed correlations to calculate Nusselt number as a function of relevant parameters. A similar problem was studied by Nag et al. [39]. They analyzed an enclosure which is adiabatic and has a perfectly conducting partition and they found that the heat transfer at the cold wall increased irrespective of the position or length of the conducting partition.

In this study, an adiabatic thin solid fin was considered as a control parameter for heat transfer and fluid flow in a triangular enclosure filled with porous medium. As can be observed from the brief literature review above, the effect of a thin fin on heat transfer in a triangular enclosure filled with porous medium has not been studied before. Thus, the study will be a useful guide for researchers and designers. In this study, the effects of dimensionless fin height, the dimensionless location of the fin, the aspect ratio of the triangle enclosure and Rayleigh number are analyzed with a Prandtl number equal to 0.71.

2. Enclosure geometry with fin

The enclosure is a right triangular enclosure filled with fluid saturated porous medium and a solid adiabatic thin fin attached at the bottom wall with height, h, as shown in Fig. 1 on the

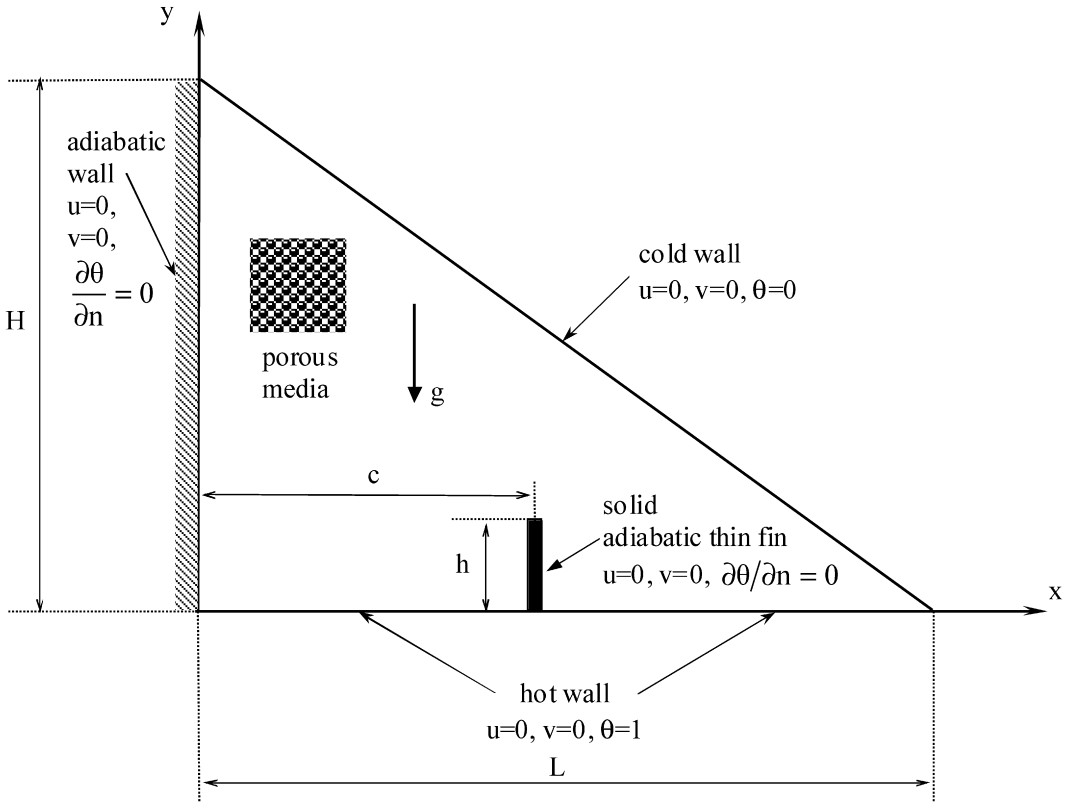

Fig. 1. Geometry of triangular enclosure with fin attached on the bottom, coordinate system and boundary conditions.

coordinate system along with the boundary condition. The temperature of the bottom wall is higher than the temperature on the inclined wall. The bottom length and height of the enclosures are depicted by L and H, respectively. An aspect ratio is defined as the ratio of the height to the length of triangular enclosure (AR $= H/L$). The distance between the origin and the fin is given by c.

3. Equations

In order to obtain governing equation of the two-dimensional laminar flow of an incompressible fluid, certain assumptions are considered as followings:

- The properties of the fluid and the porous medium are constant,
- The cavity walls are impermeable,
- The gravity acts in negative y-direction,
- Radiation heat exchange is negligible,
- The Boussinesq approximation is valid and the viscous drag and inertia terms of the momentum equations are negligible.

With these assumptions, dimensional governing equations for continuity, momentum and energy can be written as follows:

$$\frac{\partial u}{\partial x}+\frac{\partial v}{\partial y}=0 \tag{1}$$

$$\frac{\partial u}{\partial y}-\frac{\partial v}{\partial x}=-\frac{g\beta K}{\upsilon}\frac{\partial T}{\partial x} \tag{2}$$

$$u\frac{\partial T}{\partial x}+v\frac{\partial T}{\partial y}=\alpha\left(\frac{\partial^2 T}{\partial x^2}+\frac{\partial^2 T}{\partial y^2}\right) \tag{3}$$

The above equations are written in terms of the stream function defined as

$$u=\frac{\partial \psi}{\partial y},\qquad v=-\frac{\partial \psi}{\partial x} \tag{4}$$

and Eqs. (1)–(3) can be written in non-dimensional form as follows:

$$\frac{\partial^2 \Psi}{\partial X^2}+\frac{\partial^2 \Psi}{\partial Y^2}=-Ra\frac{\partial \theta}{\partial X} \tag{5}$$

$$\frac{\partial \Psi}{\partial Y}\frac{\partial \theta}{\partial X}-\frac{\partial \Psi}{\partial X}\frac{\partial \theta}{\partial Y}=\frac{\partial^2 \theta}{\partial X^2}+\frac{\partial^2 \theta}{\partial Y^2} \tag{6}$$

The non-dimensional parameters are listed as

$$X=\frac{x}{L},\qquad Y=\frac{y}{L},\qquad \theta=\frac{T-T_c}{T_h-T_c}$$

$$\Psi=\frac{\psi}{\alpha},\qquad Ra=\frac{(g\beta K(T_h-T_c)L)}{\upsilon\alpha} \tag{7}$$

3.1. Boundary conditions

Boundary conditions for the considered model are depicted on the physical model (Fig. 1). In this model, $u=v=0$ for all solid boundaries.

On the adiabatic wall

$$0<y<H,\quad \frac{\partial \theta}{\partial x}=0 \tag{8}$$

On the bottom wall

$$0<x<L,\quad \theta=1 \tag{9}$$

On the inclined wall

$$\theta=0 \tag{10}$$

On the fin

$$\frac{\partial \theta}{\partial n}=0 \tag{11}$$

Local and mean Nusselt numbers are calculated via Eqs. (12) and (13), respectively:

$$Nu_x=\left(-\frac{\partial \theta}{\partial Y}\right)_{Y=0} \tag{12}$$

$$Nu=\int_0^L Nu_x\,\mathrm{d}x \tag{13}$$

4. Solution methodology

Finite difference method is used to solve the governing equations (Eqs. (5)–(6)). Central difference method is applied to discretize the equations. The solution of linear algebraic equations was performed using the Successive Under Relaxation (SUR) method. As convergence criteria, 10^{-4} is chosen for all dependent variables and the value of 0.1 is used for the under-relaxation parameter. The number of grid points is taken as 101×101 with uniform spaced mesh in both X- and Y-directions. The numerical algorithm used in this study was tested with the classical natural convection heat transfer problem in a differentially heated square porous enclosure. The obtained numerical results are compared with those given by different authors listed in Table 1. As can be seen from the table, the obtained results show good agreement with the results of literature. Contours of the streamlines and the isotherms are almost the same as those given in literature for rectangular enclosures but they are not presented here to save space.

5. Results and discussion

The results for natural convection in triangular porous enclosure with thin solid adiabatic fin attached on the bottom wall

Table 1
Comparison of mean Nusselt number with literature at $Ra=1000$

References	Nu
Bejan [6]	15.800
Goyeau et al. [7]	13.470
Gross et al. [8]	13.448
Manole and Lage [9]	13.637
Saeid and Pop [10]	13.726
Baytas and Pop [11]	14.060
This study	13.564

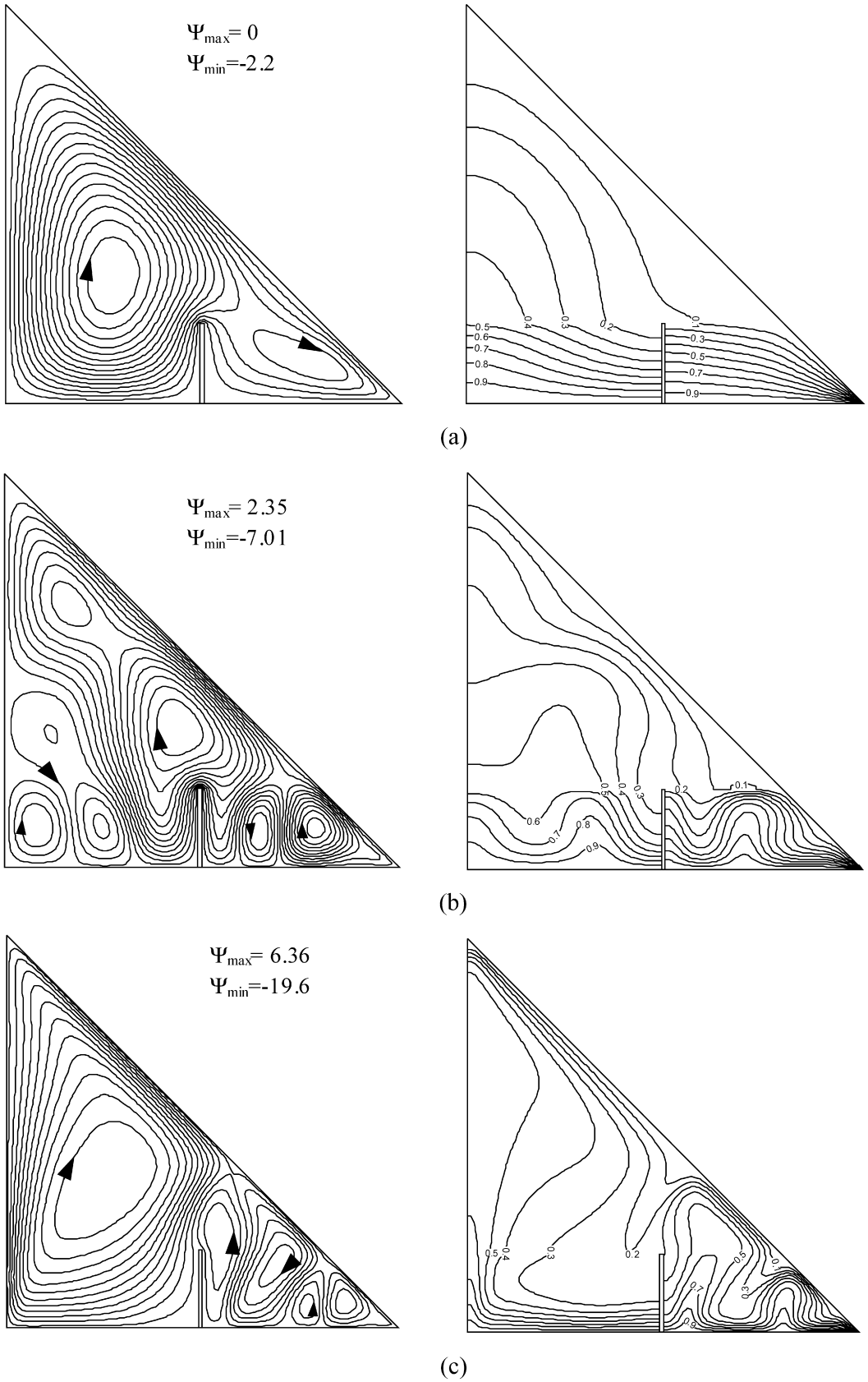

Fig. 2. Streamlines (on the left column) and isotherms (on the right column) for different Rayleigh numbers at $c = 0.5$, $h = 0.2$, AR = 1, (a) $Ra = 100$, (b) $Ra = 500$, (c) $Ra = 1000$.

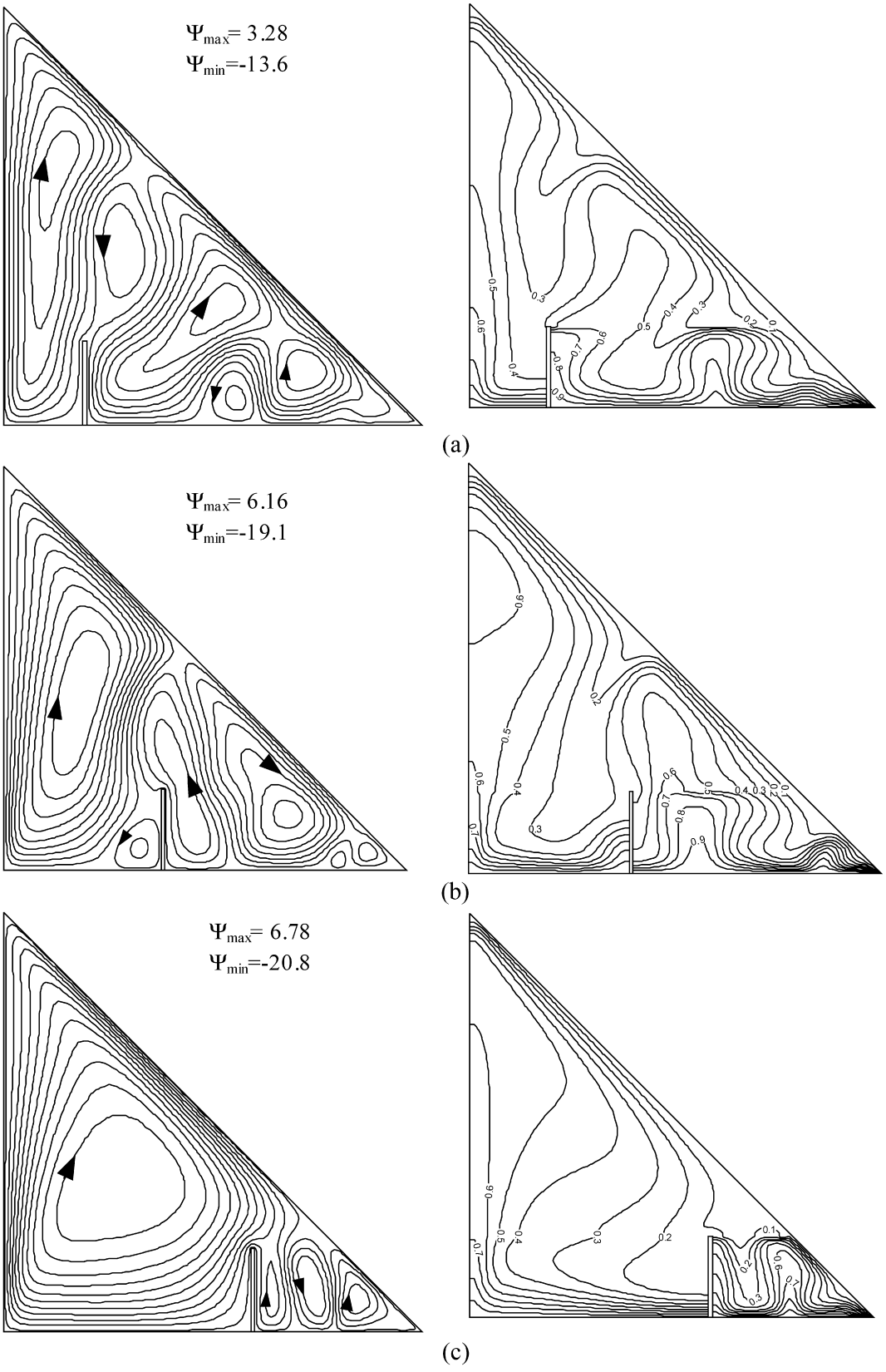

Fig. 3. Streamline (on the left column) and isotherm (on the right column) for different dimensionless fin locations at $h = 0.2$, AR $= 1$, $Ra = 1000$, (a) $c = 0.2$, (b) $c = 0.4$, (c) $c = 0.6$.

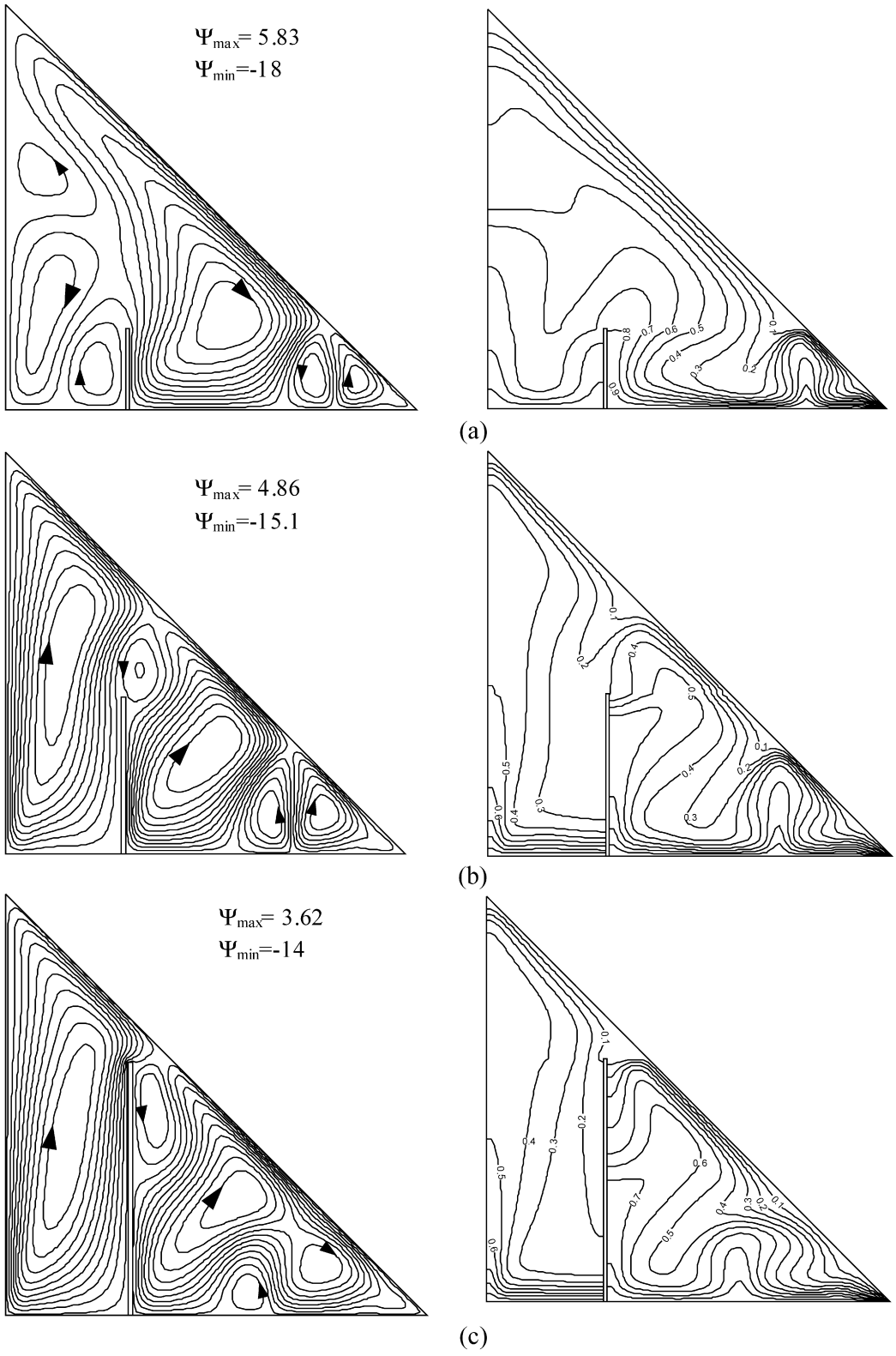

Fig. 4. Streamline (on the left column) and isotherm (on the right column) for different dimensionless fin height at $c = 0.3$, AR $= 1$, $Ra = 1000$, (a) $h = 0.2$, (b) $h = 0.4$, (c) $h = 0.6$.

is derived using the parameters as dimensionless location of the fin from 0.2 to 0.6, dimensionless height of the fin from 0.1 to 0.4, Rayleigh number from 100 to 1000 and aspect ratio of the enclosure from 0.25 to 1. Prandtl number was taken as $Pr = 0.71$.

The effects of Rayleigh number on the flow field and the temperature distribution are presented in Fig. 2(a)–(c) using streamlines (on the left) and isotherms (on the right) for $c = 0.5$, $h = 0.2$ and AR $= 1$. The graphics are arranged according to increasing Rayleigh number. Heated flow rises from the bottom

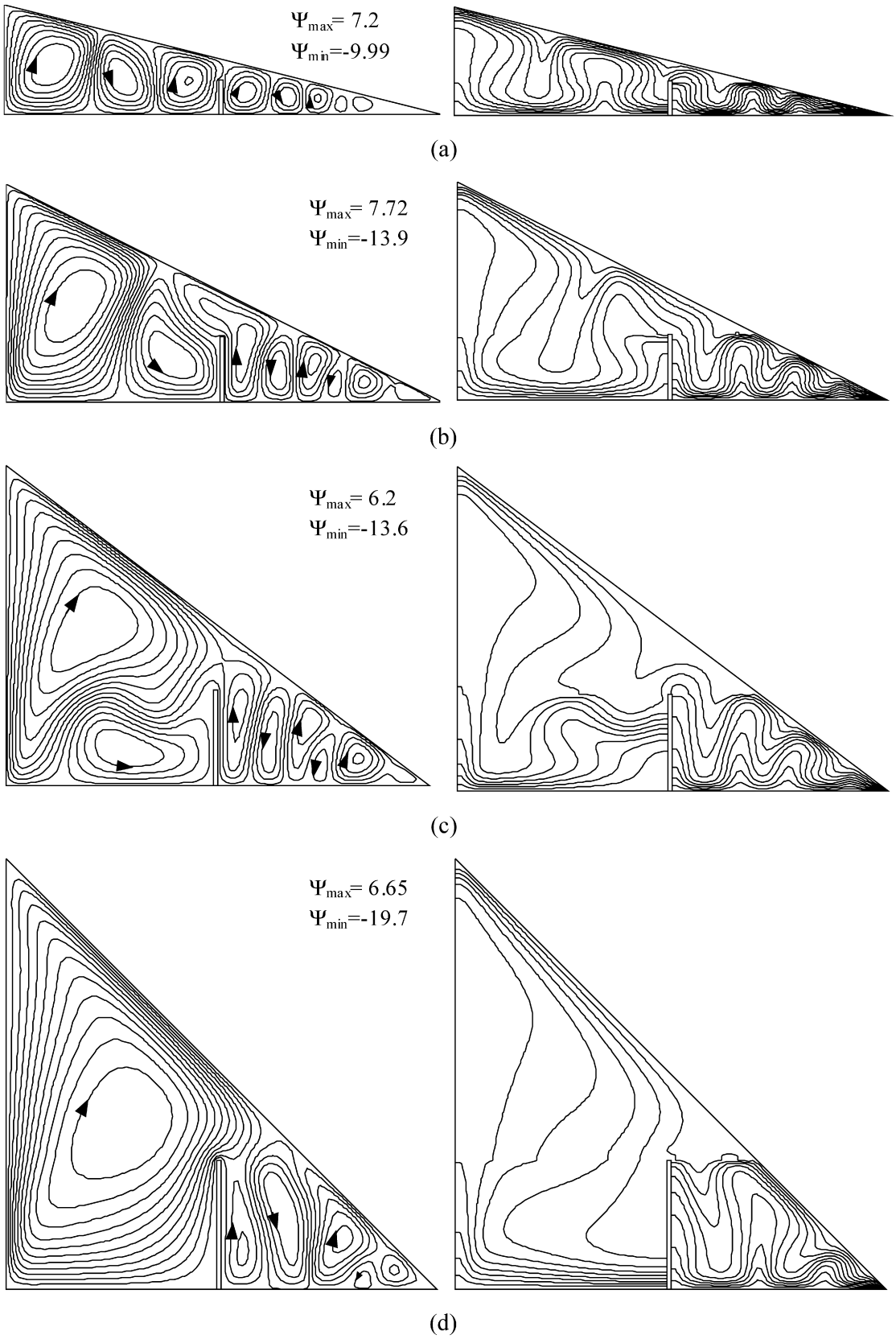

Fig. 5. Streamline (on the left column) and isotherm (on the right column) for different aspect ratios at $h = 0.3$, $c = 0.5$, $Ra = 1000$, (a) AR = 0.25, (b) AR = 0.5, (c) AR = 0.75, (d) AR = 1.

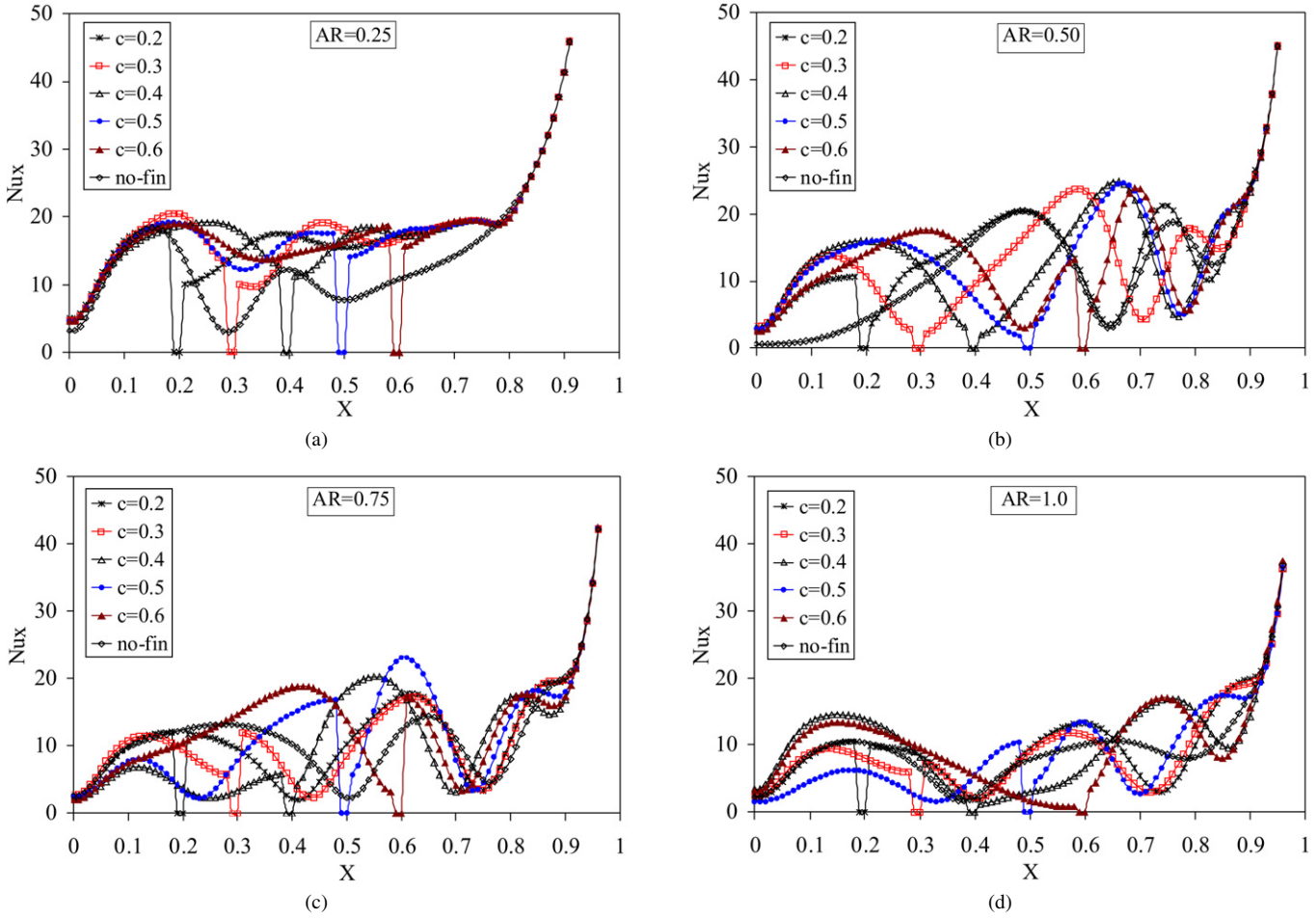

Fig. 6. Variation of local Nusselt number along the hot wall for different dimensionless fin location at $h = 0.3$, $c = 0.5$, $Ra = 500$, (a) AR = 0.25, (b) AR = 0.5, (c) AR = 0.75, (d) AR = 1.

wall, impinges to the inclined wall of the triangle and again spreads to the two sides of the thin fin. Thus, two cells are formed, one in the middle and the other on right corner of the triangle enclosure and they rotate in the clockwise direction. The strength of the cell on the corner is greater than the strength of the one in the middle due to higher local heat transfer in that part of the enclosure. The main cell is enlarged to the right corner and shows jet-like behavior between the fin and inclined wall due to constriction as given in Fig. 2(a). As Rayleigh number increases, flow field becomes more complex and streamfunctions are derived as $\psi_{\max} = 2.35$, $\psi_{\min} = -7.01$ and seven cells are formed. However, in this case there might be a transition between the quasi-conduction regime and the convection regime. For the highest Rayleigh number, the value of minimum and maximum streamfunction values increase to $\psi_{\max} = 6.36$ and $\psi_{\min} = -19.6$. A huge cell forms on the left side of the fin. This shows that the flow velocity is lower at the left part of the enclosure than the flow velocity of the right part. The intersection between hot (bottom) and cold wall (inclined) enhances the natural convection heat transfer. In other words, the flow velocity increases due to small distance between hot and cold walls. This shows that the fin is a control element for heat transfer, flow velocity and temperature distribution. The temperature distribution is represented with isotherms for the same cases as given in Fig. 2 (on the right). The isotherms become almost parallel to the bottom wall, they seem to represent conduction dominated flow field due to low Rayleigh number (Fig. 2(a)). As Rayleigh number increases, heat transfer regime changes from conduction to convection. Thus, isotherms show plume-like distribution with convection. In other words, the isotherms on the right side of the fin show a stratified flow at this high Rayleigh numbers. However, due to thin adiabatic fin, heat transfer decreases on the left part of the fin compared to the right part. The isotherms show parallel distribution to the bottom wall on the left part of fin. In other words, the fin behaves as a curtain between hot and cold walls. Fig. 3 presents the contour plots for the streamlines (on the left) and isotherms (on the right) for various values of the dimensionless location parameter of the fin for $Ra = 1000$, $h = 0.2$ and AR = 1. When the fin is located next to the vertical wall, cell centers ordered parallel to the inclined wall except for small vortices on the middle of the bottom wall as shown in Fig. 3(a). A cell rotating in the clockwise direction was observed next to the vertical wall for all values of dimensionless fin locations and the length of the cell becomes larger as the fin moves to the right corner. For $c = 0.5$, two vortices are obtained circulating in opposite directions on the left side of the fin as shown in Fig. 3(b) (on the left). The very small secondary vortex is formed at the right corner of

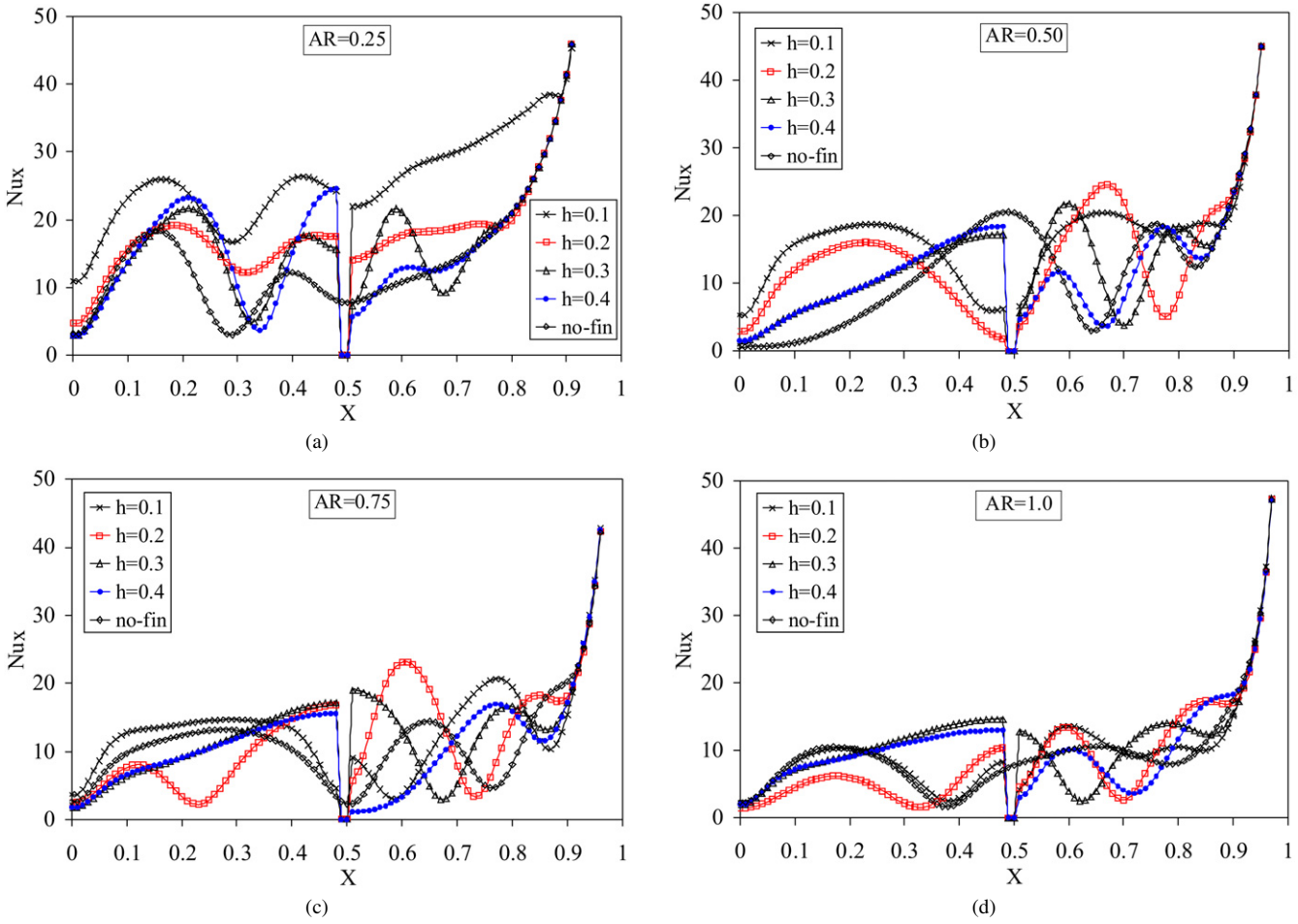

Fig. 7. Variation of local Nusselt number along the hot wall for different dimensionless fin height at $c = 0.5$, $Ra = 500$, (a) AR = 0.25, (b) AR = 0.5, (c) AR = 0.75, (d) AR = 1.

the enclosure. In this case, the flow on the left side of the fin is still cooler than the flow on the right side. When it locates to the right part of the enclosure, a huge cell forms in clockwise direction on the left side of the fin as given in Fig. 3(c) (on the left). Strong convection at the right side of the fin forms three small vortexes circulating in different directions. Finally, as seen from the streamlines, minimum streamfunction value decreases with the increase of the dimensionless location of the fin whereas the maximum streamfunction value increases. With the presence of the fin, it divides the enclosure in almost two parts both thermally and hydrodinamically, as trapezoidal and the other as a triangular enclosure. In the right part of the enclosure, strong plumelike distributions are formed and this can be observed from the isotherms in all cases as given in Fig. 3(a)–(c) (on the right). In the right part of the fins, one or two plumeshaped distribution is observed depending on the location of the fin. On the other hand, in all cases, isotherms show almost parallel distribution to the bottom wall due to long distance between hot and cold walls. It was clearly observed that with the presence of thin fin at various positions affects both flow field, and the strength of the vortexes. This is a result of the blockage effect of the fin. This result is supported by Shi and Khodadadi [38].

Fig. 4 illustrates the effects of the fin height on flow and temperature field at $Ra = 1000$, $c = 0.3$, AR = 1. For the shortest fin, three cells are formed to both sides of the fin. As fin height increases, a single big cell is formed on the left part. As heat transfer increases, it moves up to the inclined wall. Then, it impinges to the cold wall and falls, giving a rise to clockwise rotating vortex. As the fin height increases, the plumelike distribution of isotherms moves to the right corner of the triangle. This can be seen in isotherms on the right (Fig. 4(a)–(c)). As mentioned before, the fin can weaken the flow speed over the left side of the fin and thus it can decrease the expected heat transfer capacity. On the other hand, the value of the minimum streamfunction increases whereas the value of the maximum streamfunction decreases. The isotherms on the right-hand side of the fin are more closely packed than the ones in the left-hand side. This indicates that the heat transfer on the right part is better than the heat transfer on the left part. Another effective parameter on flow and temperature distribution is the aspect ratio which is defined as the height-to-base ratio (AR $= H/L$). In order to see the effect of aspect ratio clearly, the dimensionless height ratio of the fin and the dimensionless location of the fin are considered as constant for all cases and results are presented in Fig. 5. When the smallest AR is applied, the fluid at the right corner becomes motionless and a strong thermal gradient forms close to the bottom wall. Although the strength of the flow increases with the increase of AR value but multiple

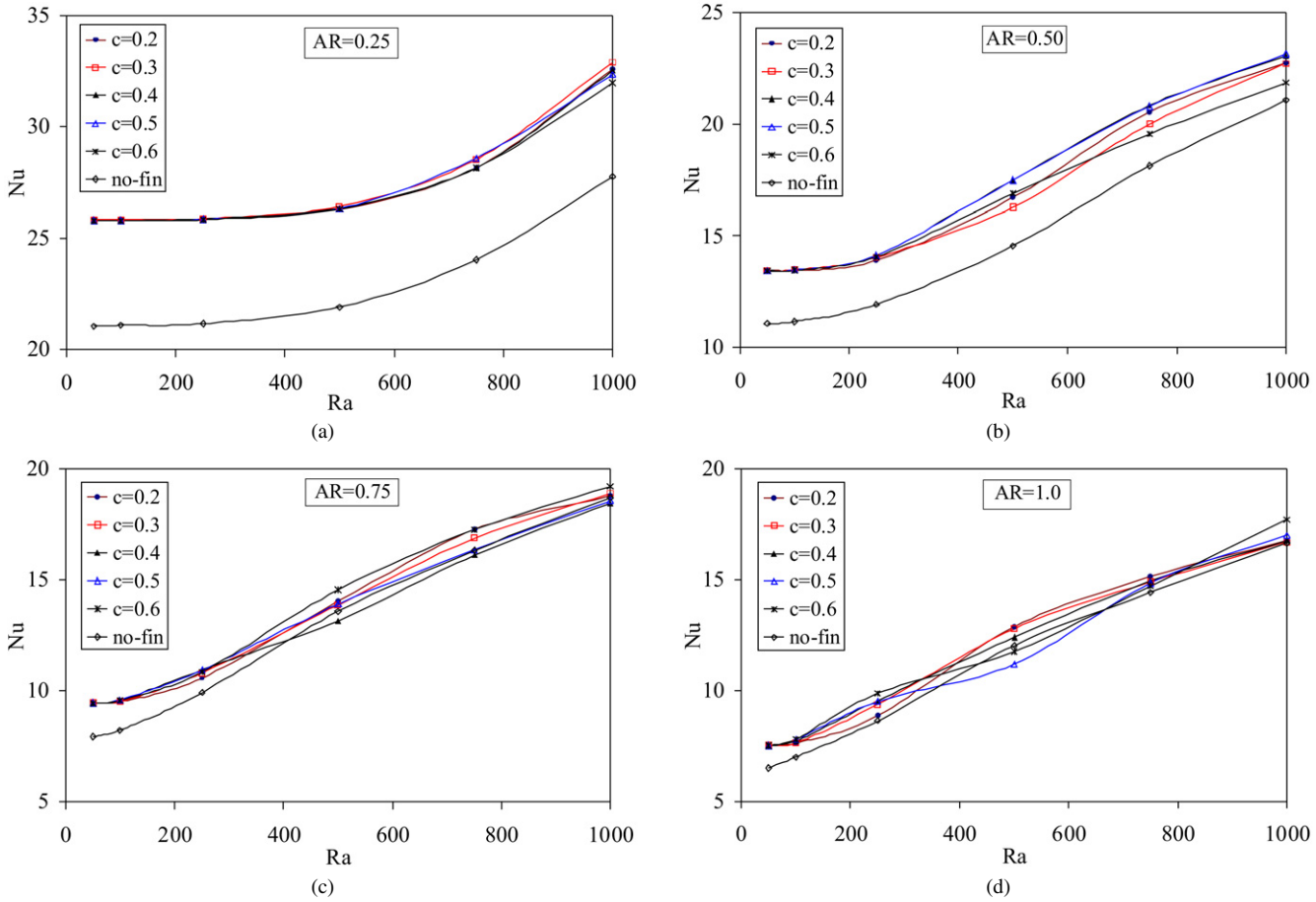

Fig. 8. Variation of mean Nusselt number with Rayleigh number for different dimensionless fin location at $h = 0.2$, (a) AR = 0.25, (b) AR = 0.5, (c) AR = 0.75, (d) AR = 1.

cells are obtained for all cases. Very small cells are obtained at the right side of the fin but number of cells decreases with the increase of AR at the left side of the fin. When AR = 1, a huge cell is obtained in clockwise at the left side of the fin. Isotherms show plumelike distribution at the right side of the fin for all cases (Fig. 5(a)–(d), on the right). However, isotherms show almost parallel distribution as AR increases due to increasing of distance between hot and cold wall, except for AR = 0.25 (Fig. 5(a)).

Variation of local Nusselt number (LNN) along the bottom wall is presented in Fig. 6(a)–(d) for different AR values and various dimensionless locations of the fin. The obtained results are compared with the results of the no-fin case to see the effects of fin insertion on heat transfer. In Fig. 6(a), it can be seen that the values of LNN are the same until the start of the fin. At the start of the fin, these show wavy variations with small amplitudes. The location of the peak values changes with different dimensionless center of location values of the fin along the bottom wall. It can be seen from the figure that higher peak values are obtained for the finned case in comparison to the no-fin case. With the increasing of AR, higher peak values are obtained when fin is close to the right corner. For the no-fin case, values are higher at the left side of the fin. This is a result of the curtain-like behavior of the adiabatic fin for the case. Convection is stronger over the right side due to the small distance between hot and cold walls. Close to the right corner of the enclosure, the effect of the fin position is not discernible. Thus, values of LNN are equal to each other. If Figs. 6(b)–(d) are compared, decrease is observed on the peak values of LNN with the increase of the value of AR. Another observation is that, if the fin is located away from the left vertical wall ($c \geqslant 0.5$), a sinusoidal trend is obtained for LNN.

Fig. 7 shows the effects of the dimensionless fin height on the distribution of LNN along the bottom wall in comparison to no-fin case while the fin is attached on the middle of the bottom wall. It can be seen from the figure that, the sinusoidal variation is formed for both left and right side of the fin due to presence of vortexes. The peak values of LNN decrease as the dimensionless fin height increases for AR = 0.25 (Fig. 7(a)). When AR = 0.5, LNN values increase monotonically till the start of the fin for the case of $h = 0.4$, 0.3 and no-fin. However, for the smaller dimensionless fin height values, LNN shows parabolic variation. As we observed earlier, the fin obstructs the heat transfer between left and right sides of the fin. The highest peak value is obtained at $h = 0.2$. When AR = 0.75 and AR = 1, trend of the LNN shows the similar variation. On the contrary of other cases, peak value of LNN is decreased for AR = 1 for $h = 0.2$ due to increasing volume of the enclosure. Fig. 8(a)–(d) shows the effects of AR and dimensionless location of the fin on mean Nusselt number. For small Rayleigh

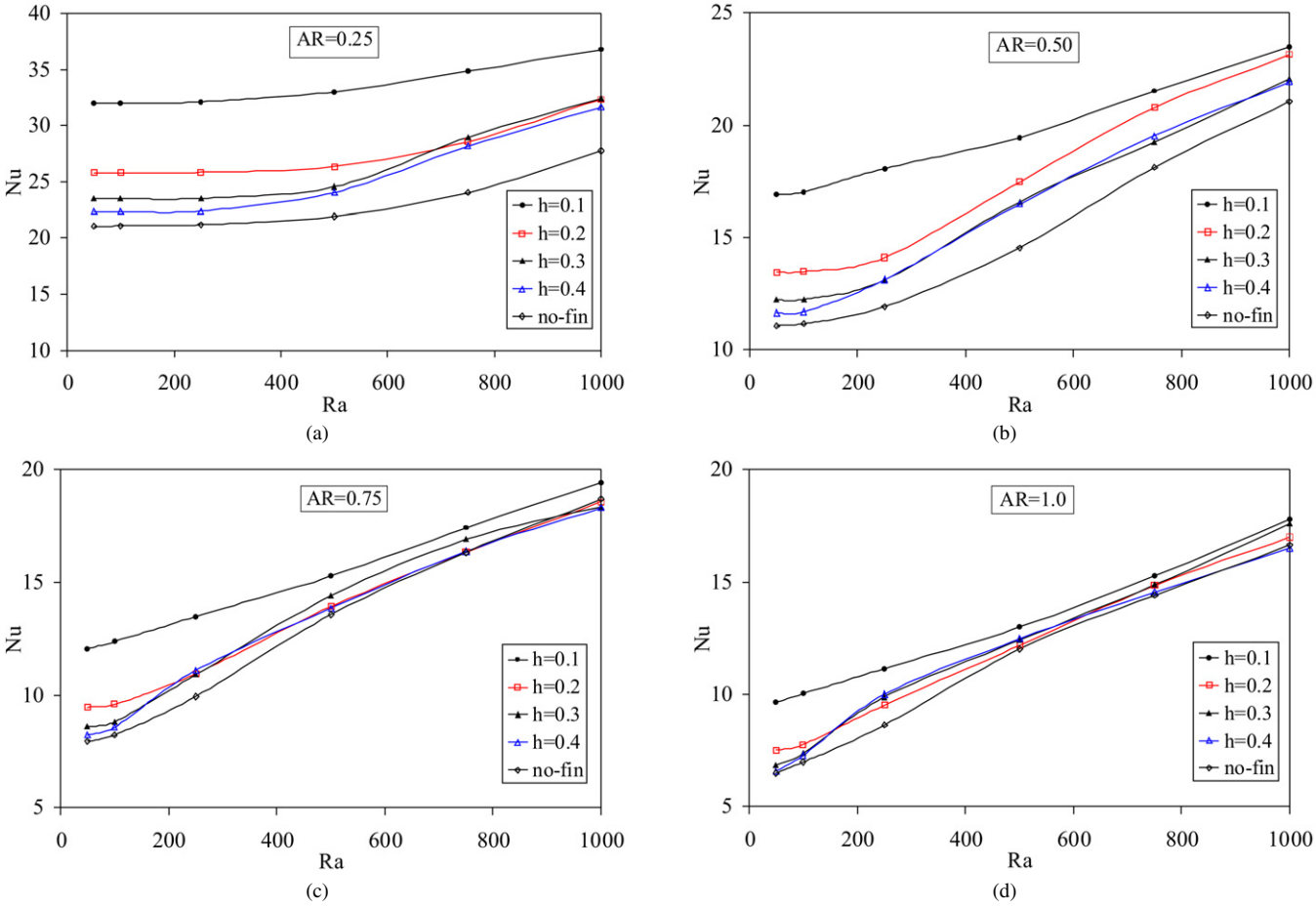

Fig. 9. Variation of mean Nusselt number with Rayleigh number for different dimensionless fin height at $c = 0.5$, (a) AR = 0.25, (b) AR = 0.5, (c) AR = 0.75, (d) AR = 1.

numbers, *Nu* number values are almost equal to each other due to quasi-conductive regime. However, as can be expected, these values increase as *Ra* number increases. For the smallest AR value of the enclosure, the location of the fin is not effective on heat transfer. However, presence of the fin enhances the heat transfer when it is compared to the no-fin case (Fig. 8(a)). As AR increases, the heat transfer difference between the finned enclosure and no-fin case decreases. Dimensionless location of the fin plays an important role for higher Rayleigh numbers. Heat transfer increases when the fin is close to the vertical wall. When AR = 0.75 and AR = 1.0 as is shown in Fig. 8(c) and (d), the heat transfer decreases especially for higher Rayleigh numbers as a result of the fin.

The value of the mean Nusselt number as a function of the aspect ratio and dimensionless fin height are presented in Fig. 9(a)–(d) for $c = 0.5$. The variations of the mean Nusselt number are shown for different Rayleigh numbers. In Fig. 9(a), the value of the mean Nusselt number is constant up to $Ra = 500$ as a result of the increase in conductive heat transfer regime. As the dimensionless fin height increases, the value of the mean Nusselt number decreases. When the values are compared to the values in the no-fin case, it is concluded that the addition of the fin enhances heat transfer. As AR increases, convection heat transfer regime becomes dominant over the conduction regime and the value of mean Nusselt number increases as Rayleigh number increases. However, the effects of the fin height decrease as the aspect ratio increases.

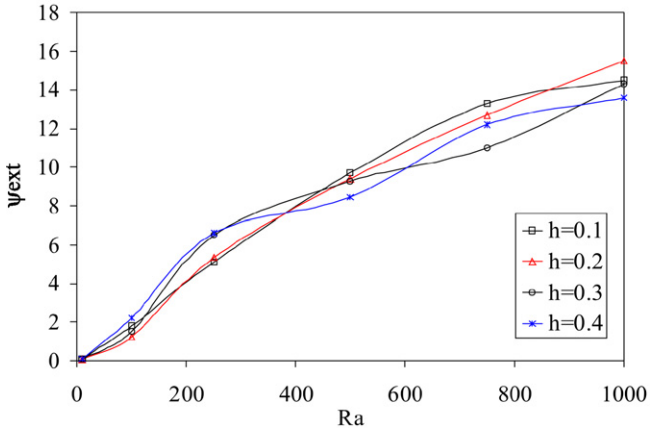

Fig. 10. Effects of dimensionless fin height on extreme stream-function values as a function of Rayleigh number at AR = 1 and $c = 0.25$.

Fig. 10 shows the effects of the dimensionless fin height and the Rayleigh number on the extreme streamfunction values for AR = 1 and $c = 0.25$. As Rayleigh number increases, the convection heat transfer regime also increases as a re-

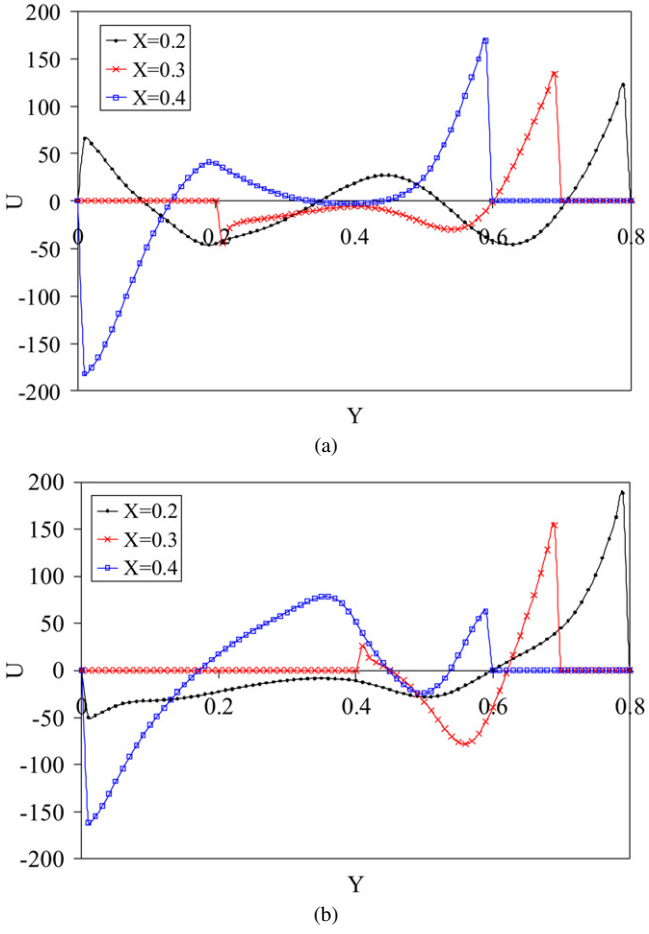

Fig. 11. Velocity profiles at different stations on the bottom wall of enclosure at AR = 1, $c = 0.3$ and $Ra = 1000$, (a) $h = 0.2$, (b) $h = 0.4$.

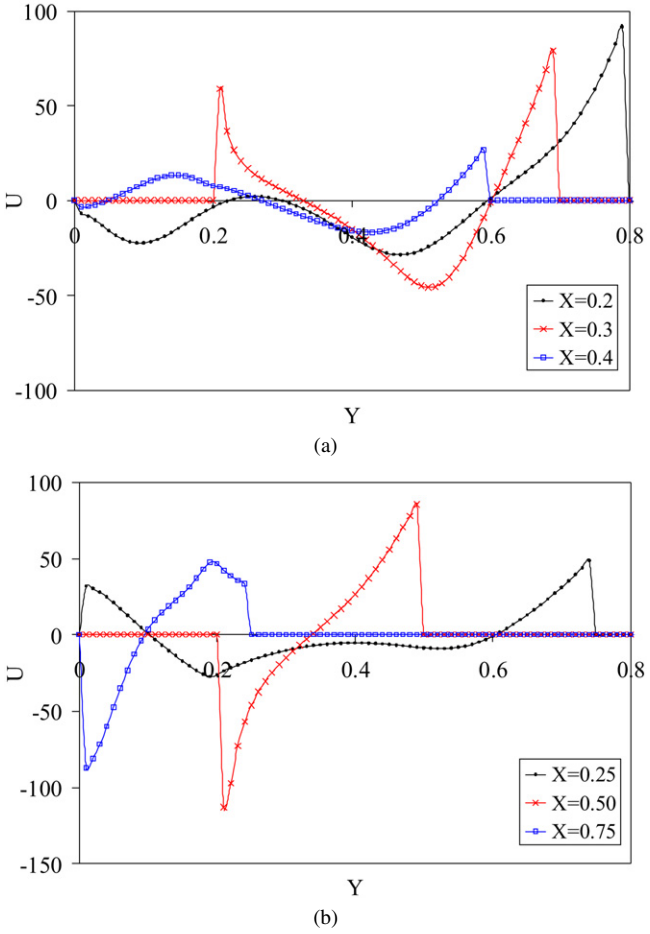

Fig. 12. Velocity profiles at different stations on the bottom wall of enclosure at AR = 1, $h = 0.2$ and Ra = 500, (a) $c = 0.3$, (b) $c = 0.5$.

sult of the increases in the buoyancy forces. As dimensionless fin height increases, the value of extreme stream-function decreases since increasing of the partition height presents an obstacle for flow field. This observation is supported by Ben-Nakhi and Chamkha [30]. However, the values of smaller Rayleigh number and the values of extreme stream-function do not follow this trend due to quasi-conductive regime.

Finally, to show the effects of the dimensionless fin height and dimensionless fin location on flow field, we have presented the vertical velocity profiles in Fig. 11 and Fig. 12, respectively, for $Ra = 1000$. Results are illustrated at $X = 0.2, 0.3$ and 0.4. As given in figures, velocity profiles show wavy trend almost in all cases. Regarding the comparison between Fig. 11(a) and (b), it is shown that, the velocity values close to the bottom wall and the inclined wall increase as the fin height increases. On the other hand, velocities are higher in the middle of the enclosure and they become smaller near the vertical wall of the enclosure than that of right corner. As can be seen also from the figures, negative velocities are formed due to flow reversal. This phenomenon can be explained through the streamlines on the left side of Figs. 2–5 that heated fluid moves from hot wall to cold and from impinged to inclined wall and dispersed. Therefore, the movement caused positive and negative velocities.

Fig. 12 can be compared with Fig. 11 for using $c = 0.3$, $h = 0.2$ and AR = 1 and using different Rayleigh numbers. It is clearly shown in the figure, for $Ra = 500$, that the velocity values are very small due to the effect of the low Rayleigh number. When Fig. 12(a) and (b) are compared, it can be seen that the dimensionless location of the fin has important effect on the flow field. The trend of the velocity profiles completely changes as the dimensionless location of the fin changes.

6. Conclusion

Natural convection heat transfer and fluid flow in porous triangular enclosures with vertical solid adiabatic thin fin have been numerically analyzed for the dimensionless location of the fin from 0.2 to 0.6, dimensionless height of the fin from 0.1 to 0.4, Rayleigh number from 100 to 1000 and aspect ratio from 0.25 to 1.

Important observations from the solutions are listed as follows:

(1) Placing an adiabatic solid vertical thin fin on the bottom wall generally modifies the clockwise rotating main vortex near the left vertical adiabatic wall. The dimensionless

height of the fin, Rayleigh number and dimensionless location of the fin change its location and length.

(2) Nusselt number is an increasing function of Rayleigh number but it can be constant at very small Rayleigh numbers due to domination of quasi-conductive heat transfer regime.

(3) Dimensionless location of the fin changes the number of vortexes and enhances the strength of the flow.

(4) With the increasing of dimensionless fin height, the fin makes blockage effects for the flow at the left side of the fin. Thus, heat transfer decreases.

(5) Wavy variation is obtained for local Nusselt number along the bottom wall. The values of local and mean Nusselt numbers are decreased with the increasing of AR.

(6) It was noted that the fin can be a passive control parameter for heat transfer and fluid flow.

References

[1] D.A. Nield, A. Bejan, Convection in Porous Media, second ed., Springer, NY, 2006.

[2] D.B. Ingham, I. Pop, Transport Phenomena in Porous Media II, Pergamon, 2005.

[3] G. De Vahl Davis, Natural convection of air in a square cavity: A benchmark numerical solution, Int. J. Numer. Methods Fluids 3 (1983) 249–264.

[4] I. Catton, Natural convection in enclosures, in: Proc. 6th Int. Heat Transfer Conf. 6, 1978, pp. 13–31.

[5] S. Ostrach, Natural convection in enclosures, Adv. Heat Transfer 8 (1972) 161–227.

[6] A. Bejan, On the boundary layer regime in a vertical enclosure filled with a porous medium, Lett. Heat Mass Transfer 6 (1979) 93–102.

[7] B. Goyeau, J.P. Songbe, D. Gobin, Numerical study of double-diffusive natural convection in a porous cavity using the Darcy–Brinkman formulation, Int. J. Heat Mass Transfer 39 (1996) 1363–1378.

[8] R.J. Gross, M.R. Bear, C.E. Hickox, The application of flux-corrected transport (FCT) to high Rayleigh number natural convection in a porous medium, in: Proc. 8th Int. Heat Transfer Conf., San Francisco, CA, 1986.

[9] D.M. Manole, J.L. Lage, Numerical benchmark results for natural convection in a porous medium cavity, in: Heat Mass Transfer Porous Media, ASME Conf., 1992, pp. 55–60.

[10] N.H. Saeid, I. Pop, Natural convection from a discrete heater in a square cavity filled with a porous medium, J. Porous Media 8 (2005) 55–63.

[11] A.C. Baytas, I. Pop, Free convection in a square porous cavity using a thermal nonequilibrium model, Int. J. Thermal Sci. 41 (2002) 861–870.

[12] H. Asan, L. Namli, Laminar natural convection in a pitched roof of triangular cross-section: Summer day boundary conditions, Energy and Buildings 33 (2000) 69–73.

[13] H. Asan, L. Namli, Numerical simulation of buoyant flow in a roof of triangular cross section under winter day boundary conditions, Energy and Buildings 33 (2001) 753–757.

[14] S.C. Tzeng, J.H. Liou, R.Y. Jou, Numerical simulation-aided parametric analysis of natural convection in a roof of triangular enclosures, Heat Transfer Engrg. 26 (2005) 69–79.

[15] V.A. Akinsete, T.A. Coleman, Heat transfer by steady laminar free convection in triangular enclosures, Int. J. Heat Mass Transfer 25 (1982) 991–998.

[16] Y.E. Karyakin, Y.A. Sokovishin, O.G. Martynenko, Transient natural convection in triangular enclosures, Int. J. Heat Mass Transfer 31 (1988) 1759–1766.

[17] Y. Varol, A. Koca, H.F. Oztop, Natural convection in a triangle enclosure with flush mounted heater on the wall , Int. Comm. Heat Mass Transfer 33 (2006) 951–958.

[18] Y. Varol, H.F. Oztop, A. Varol, Free convection in porous media filled right-angle triangular enclosures, Int. Comm. Heat Mass Transfer 33 (2006) 1190–1197.

[19] A.C. Baytas, I. Pop, Free convection in oblique enclosures filled with a porous medium, Int. J. Heat Mass Transfer 42 (1999) 1047–1057.

[20] A.C. Baytas, I. Pop, Natural convection in a trapezoidal enclosure filled with a porous medium, Int. J. Engrg. Sci. 39 (2001) 125–134.

[21] B.V.R. Kumar, B. Kumar, Parallel computation of natural convection in trapezoidal enclosures, Math. Comp. Sim. 65 (2004) 221–229.

[22] Y. Varol, A. Koca, H.F. Oztop, Laminar natural convection in saltbox roofs for both summerlike and winterlike boundary conditions, J. Appl. Sci. 6 (2006) 2617–2622.

[23] F. Moukalled, S. Acharya, Natural convection in a trapezoidal enclosure with offset baffles, J. Them. Heat Transfer 15 (2001) 212–218.

[24] Y. Varol, A. Koca, H.F. Oztop, Natural convection heat transfer in Gambrel roofs, Building Environment 42 (2007) 1291–1297.

[25] P.V.S.N. Murthy, B.V.R. Kumar, P. Singh, Free convection heat transfer from a horizontally wavy surface in a porous enclosure, Numer. Heat Transfer Part A 31 (1997) 207–221.

[26] Y. Varol, H.F. Oztop, Free convection in a shallow wavy enclosure, Int. Comm. Heat Mass Transfer 33 (2006) 764–771.

[27] H. Turkoglu, N. Yucel, Effect of heater and cooler locations on natural convection in square cavities, Numer. Heat Transfer Part A 27 (1995) 351–358.

[28] E. Zimmerman, S. Acharya, Free convection heat transfer in a partially divided vertical enclosure with conducting end walls, Int. J. Heat Mass Transfer 30 (1987) 319–331.

[29] I. Dagtekin, H.F. Oztop, Natural convection heat transfer by heated partitions within enclosure, Int. Comm. Heat Mass Transfer 28 (2001) 823–834.

[30] A. Ben-Nakhi, A.J. Chamkha, Natural convection in inclined partitioned enclosures, Heat Mass Transfer 42 (2006) 311–321.

[31] M. Hasnaoui, E. Bilgen, P. Vasseur, Natural convection above an array of open cavities heated from below, Numer. Heat Transfer Part A 18 (1990) 436–482.

[32] N. Yucel, A.H. Ozdem, Natural convection in partially divided square enclosure, Heat Mass Transfer 40 (2003) 167–175.

[33] I. Dagtekin, H.F. Oztop, M. Inalli, A numerical analysis of natural convection in a rectangular channel partly divided by thin plates, in: The 6th National Meeting on Cooling and Air Conditioning Techniques (SIMER), Adana, 2000 (in Turkish).

[34] P.L. Oosthuizen, J.T. Paul, Free convection heat transfer in a cavity fitted with a horizontal plate on the cold wall, in: S.M. Shenkman, et al. (Eds.), Advances in Enhanced Heat Transfer, vol. 43, 1985, pp. 101–107.

[35] E. Bilgen, Natural convection in an inclined with partial partitions, Renewable Energy 26 (2002) 257–270.

[36] S.H. Tasnim, M.R. Collins, Numerical analysis of heat transfer in a square cavity with a baffle on the hot wall, Int. Comm. Heat Mass Transfer 31 (2004) 639–650.

[37] E. Bilgen, Natural convection in cavities with a thin fin on the hot wall, Int. J. Heat Mass Transfer 48 (2005) 3493–3505.

[38] X. Shi, J.M. Khodadadi, Laminar convection heat transfer in a differentially heated square cavity due to a thin fin on the hot wall, J. Heat Transfer 125 (2003) 624–634.

[39] A. Nag, A. Sarkar, V.M.K. Sastri, Natural convection in a differentially heated square cavity with a horizontal partition plate on the hot wall, Comput. Methods Appl. Mech. Engrg. 110 (1993) 143–156.